Selective Range Iterative Adaptive Approach for High-Resolution DOA Estimation

YUAN CHEN[1], LONG-TING HUANG [iD][2], AND HING CHEUNG SO [iD][3], (Fellow, IEEE)
[1]School of Computer and Communication Engineering, University of Science and Technology Beijing, Beijing 100083, China
[2]School of Information Engineering, Wuhan University of Technology, Wuhan 430070, China
[3]Department of Electronic Engineering, City University of Hong Kong, Hong Kong

Corresponding author: Long-Ting Huang (huanglt08@whut.edu.cn)

ABSTRACT In this paper, the problem of direction-of-arrival (DOA) estimation for a uniform linear array with single-snapshot observations is addressed. Two non-parametric DOA estimators are developed, which can be applied in any azimuth range with one snapshot. Their main idea is iteratively updating the DOA estimates using the weighted least squares and covariance matrix. Two criteria for implementing the covariance matrix are devised, which guarantee high resolution of the proposed methods. The simulation results are included to demonstrate the superiority of our algorithms over several conventional DOA methods in terms of both estimation performance and computational complexity.

INDEX TERMS Direction-of-arrival, single snapshot, iterative adaptive approach, selective azimuth range, weighted least squares.

I. INTRODUCTION

Direction-of-arrival (DOA) estimation is an important research topic in sensor array processing and can be applied in many areas such as radar, sonar and communications [1]–[3]. It refers to accurately determining the locations of sources using a finite set of noisy measurements by means of either parametric or non-parametric methodologies [4]. In the parametric approach, the signal is assumed to be described as a known function, which allows the derivation of the optimal estimators. Nevertheless, the performance of parametric methods deteriorates if the assumed signal model and actual one are mismatched. While for the non-parametric method, there is no assumption on the signal, and therefore, it can be utilized in many applications even when there is no prior knowledge of the signal.

Among numerous non-parametric estimators developed in the literature, one representative methodology is the classical delay-and-sum (DAS) method [5], where the observed data are weighted and time-shifted for different scanning azimuth ranges in the space $[0°, 180°)$. However, this method has high sidelobe, leading to poor resolution in the case of two closely-spaced source waveforms. To improve the performance, several algorithms such as principal-singular-vector utilization

for modal analysis (PUMA) [6], Capon [7]–[9], multiple signal classification (MUSIC) [10]–[12] have been proposed, which can provide high-resolution in the scenario of high signal-to-noise ratio (SNR) and large number of snapshots. In [13]–[15], amplitude and phase estimator (APES) was suggested to accurately estimate the power of the source signal, which can resolve sources as well. Although these methods can obtain high accurate DOA estimation in the case of high SNR or numerous snapshots, their performance degrades when only a few snapshots are available. This is because that accurate implementation of covariance matrix in these methods requires a large number of snapshots.

Furthermore, in real-world applications, single snapshot is commonly encountered, when the environment around the sensors does not change in a short duration. Moreover, in wireless communications, single-input single-output (SISO) [16], [17] and/or multiple-input single-output (MISO) radar/sonar range-Doppler imaging [18], the mathematical model of observations aligns with that of uniform linear array (ULA) using single snapshot. Since the developed estimators such as Capon, MUSIC and APES estimators, cannot provide a satisfactory performance, the problem of DOA estimation for single snapshot has attracted considerable attention.

In [19]–[21], a super-resolution method, namely, the iterative adaptive approach (IAA), is developed, which iteratively

The associate editor coordinating the review of this manuscript and approving it for publication was Xianpeng Wang.

obtaining DOA estimates using the weighted least squares (WLS) approach. According to the Markov estimate [22], [23], the weighing matrix in IAA is in fact the covariance matrix of observations. To ensure the high resolution, IAA updates the covariance matrix using the DOA estimate iteratively, and hence, accurate implementation of the IAA covariance matrix requires the estimates in full azimuth ranges of $[0°, 180°)$. That is to say, IAA can only work well in the fixed azimuth range. However, in the case that the coarse arrival ranges of sources are known *a priori*, full azimuth estimation of IAA is redundant and suffers from high computational cost. Although fast implementation of IAA [24]–[26] has been proposed, it is still not a good choice for selective range DOA estimation.

In this paper, we address the DOA estimation problem in a selective azimuth range, where ULA is taken as an illustration. Two high-resolution estimators, referred to as selective IAA I (SIAA I) and selective IAA II (SIAA II), are devised, which are realized according to the IAA cost function. To be employed in any selective azimuth range, two implementation criteria of the covariance matrix are suggested, where only the DOA estimates in the interested azimuth range is required. For SIAA I, we divide the full azimuth range into interested one and non-interested one. Then the covariance matrix is modified utilizing the DOA estimates in the interested range as well as the variance estimates outside the selective range that can be obtained by the selective DOA estimates. While in SIAA II, we redefine the mathematical model of observations as the noise-free and noisy component, where the former is described by the selective azimuth range. The covariance matrix of SIAA II is then defined by the DOA estimates and the variance of noise term.

The rest of this paper is organized as follows. In Section II, the ULA signal model and a brief review of IAA algorithm are given. In Section III, we present the main idea of SIAA I, where the derivation of noise variance is suggested. The SIAA II is also developed, and the computational costs of both SIAA I and SIAA II are provided. Computer simulations in Section IV demonstrate that the proposed methods perform better than the Capon, APES and MUSIC estimators. Finally, conclusions are drawn in Section V.
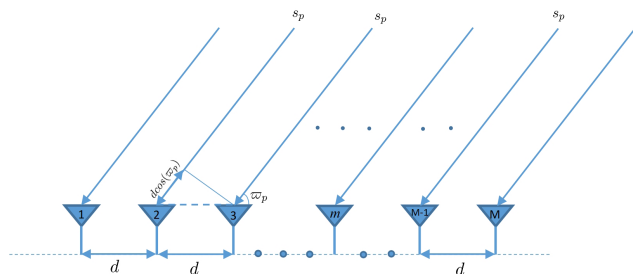

FIGURE 1. Illustration of uniform linear array.

II. REVIEW OF IAA

As shown in Figure 1, we consider a ULA [27] with M well-calibrated and identically-polarized sensors. Suppose in the far-field, there are P uncorrelated narrowband source targets,

say, s_1, s_2, $\cdots$ s_P. It is worth pointing out that we take s_p as an illustration in Figure 1. Without loss of generality, the observed signal of the mth sensor at time t, denoted by $y_m(t)$, is modeled as:

$$y_m(t) = \sum_{p=1}^{P} s_p(t) e^{-j2\pi md \cos(\varpi_p)/\lambda} + q_m(t),$$
$$m = 1, 2, \cdots, M \quad (1)$$

where $s_p(t)$ is the waveform impinging on the ULA plane at time t, $\varpi_p \in [0°, 180°)$ denotes the azimuth angle corresponding to the pth source and λ is the wavelength. The q_m denotes the noise term which is independent and identically distributed (IID) complex random variable following the zero-mean white Gaussian distribution with unknown variance σ^2. The task of DOA estimation is finding $\{\varpi_p\}_{p=1}^{P}$ from observations $\{y_m(t)\}_{m=1}^{M}$. Note that d in Figure 1 denotes the distance between two adjacent sensors, which is chosen as $\lambda/2$ [28].

In the following, we consider the single-snapshot DOA estimation problem. It is noted that our study can also be extended to the multiple snapshots. We first review the one-dimensional IAA [19], which can provide the high-resolution full range DOA estimation for the single snapshot data.

The observations in (1) is rewritten in vector form:

$$\mathbf{y}_M = \mathbf{A}_{M \times L} \mathbf{x}_L, \quad (2)$$

where $\mathbf{y}_M = [y_1 \ y_1 \ \cdots \ y_M]^T$ is observation vector with T denoting the transpose operator, and $\mathbf{x}_L = [x_1 \ x_2 \ \cdots \ x_L]^T$ with $L \geq M$, $\mathbf{A}_{M \times L} = [\mathbf{a}_M(\theta_1) \ \mathbf{a}_M(\theta_2) \ \cdots \ \mathbf{a}_M(\theta_L)]$ with

$$\mathbf{a}_M(\theta_l) = [e^{-j\pi \cos(\theta_1)} \ e^{-j2\pi \cos(\theta_l)} \ \cdots \ e^{-jM\pi \cos(\theta_l)}]^T. \ (3)$$

Here, the azimuth range $[0°, 180°)$ is divided into L uniform grid points $\{\theta_l\}_{l=1}^{L}$, while x_l and $\mathbf{a}_M(\theta_l)$ ($l = 1, 2, \cdots, L$) are the amplitude and frequency-vector associated with θ_l, respectively. Assuming that L is chosen sufficiently large and in the absence of noise, we have:

$$x_l = \begin{cases} s_p, & \theta_l = \varpi_p, \quad p = 1, 2, \cdots, P \\ 0, & \text{otherwise.} \end{cases} \quad (4)$$

The conceptual estimate of x_l, denoted by $\hat{x}_l$, can be obtained by the WLS approach with the cost function

$$J(x_l) = (\mathbf{y}_M - \mathbf{a}_M(\theta_l)x_l)^H \mathbf{W}_l^{-1} (\mathbf{y}_M - \mathbf{a}_M(\theta_l)x_l), \quad (5)$$

where $^{-1}$ and ^{H} denote matrix inverse and conjugate transpose, respectively. Employing the criterion in the Markov estimates [23], the weighting matrix $\mathbf{W}_l$ for each x_l is:

$$\mathbf{W}_l = E\{(\mathbf{y}_M - \mathbf{a}_M(\theta_l)x_l) (\mathbf{y}_M - \mathbf{a}_M(\theta_l)x_l)^H\}$$
$$= \mathbf{Q}_M - E\{|x_l|^2\}\mathbf{a}_M(\theta_l)\mathbf{a}_M^H(\theta_l), \quad (6)$$

where $E\{\cdot\}$ denotes the expectation operator,

$$\mathbf{Q}_M = E\{\mathbf{y}_M \mathbf{y}_M^H\}$$
$$= \mathbf{A}_{M \times L} \text{diag}\left(E\{|x_1|^2\} \ E\{|x_2|^2\} \ \cdots \ E\{|x_L|^2\}\right) \mathbf{A}_{M \times L}^H, \quad (7)$$

is the covariance matrix with diag $(\cdot)$ denoting the diagonal matrix. Since the expectation in $\mathbf{Q}_M$ is hard to obtain, we assume $E\{|x_l|^2\} \approx |x_l|^2$. In this case, $\mathbf{Q}_M$ can be regarded as a complicated function of x_l, therefore, (5) is usually solved in an iterative manner.

Employing the Woodbury matrix identity [29], $\mathbf{W}_l$ can be replaced by $\mathbf{Q}_M$ and the $(\ell+1)$th estimate, referred to as $\hat{x}_l^{(\ell+1)}$, is

$$
\begin{aligned}
\hat{x}_l^{(\ell+1)} &= \arg \min_{\tilde{x}_l} J(\tilde{x}_l) \\
&= \frac{\mathbf{a}_M^H(\theta_l)(\mathbf{Q}_M^{(\ell)})^{-1}\mathbf{y}_M}{\mathbf{a}_M^H(\theta_l)(\mathbf{Q}_M^{(\ell)})^{-1}\mathbf{a}_M(\theta_l)}, \quad l = 1, 2, \cdots, L, \quad (8)
\end{aligned}
$$

where

$$
\mathbf{Q}_M^{(\ell)} = \mathbf{A}_{M \times L} \mathrm{diag}\left(|\hat{x}_1^{(\ell)}|^2 \; |\hat{x}_2^{(\ell)}|^2 \; \cdots \; |\hat{x}_L^{(\ell)}|^2\right) \mathbf{A}_{M \times L}^H. \quad (9)
$$

III. PROPOSED METHOD

As it is discussed in (8) in Section II, the inverse operation of the covariance matrix $\mathbf{Q}_M$ is required in each iteration. According to (9), the $\mathbf{Q}_M$ is defined by using the spectrum of full azimuth range. In the applications that only a selective azimuth range, e.g., $(\vartheta_1, \vartheta_2)$ with $0° < \vartheta_1 < \vartheta_2 < 180°$, is interested in, IAA still needs to calculate the full range spectrum due to the requirement of implementing $\mathbf{Q}_M$. Since IAA is a type of grid search method, it suffers from the high computational cost for full spectrum estimation. Therefore, IAA cannot be directly applied to the DOA estimation in a selective range.

As the covariance matrix $\mathbf{Q}_M$ is a key of IAA, in this section, we develop two implementation methods and propose two generalized IAA versions accordingly.

A. SIAA I

Suppose all signals are located in our interested ranges $[\vartheta_1, \vartheta_2]$. Then the mathematical model in (2) can be rewritten as:

$$
\mathbf{y}_M = \mathbf{A}_{M \times L}(\mathbf{u} + \mathbf{v}), \quad (10)
$$

where $\mathbf{u}$ corresponds to the spectrum in $(\vartheta_1, \vartheta_2]$, while $\mathbf{v}$ is the spectrum of $[0°, \vartheta_1]$ and $(\vartheta_2, 180°)$. According to our assumption, all source directions are located in $(\vartheta_1, \vartheta_2]$. Therefore, $\mathbf{v}$ can be regarded as the noise term in frequency domain.

It is assumed that $(\vartheta_1, \vartheta_2]$ is uniformly divided into K bins. Then the requirement of $180/L = (\vartheta_2 - \vartheta_1)/K$ should be satisfied. Under this assumption, (10) can be expressed as

$$
\mathbf{y}_M = \mathbf{B}_{M \times K} \mathbf{u}_K + \mathbf{C}_{M \times S} \mathbf{v}_S, \quad (11)
$$

where $S = L - K$ and

$$
\mathbf{B}_{M \times K} = \begin{bmatrix}
e^{-j\pi \cos(\omega_1)} & e^{-j\pi \cos(\omega_2)} & \cdots & e^{-j\pi \cos(\omega_K)} \\
e^{-j2\pi \cos(\omega_1)} & e^{-j2\pi \cos(\omega_2)} & \cdots & e^{-j2\pi \cos(\omega_K)} \\
\vdots & \vdots & \ddots & \vdots \\
e^{-jM\pi \cos(\omega_1)} & e^{-jM\pi \cos(\omega_2)} & \cdots & e^{-jM\pi \cos(\omega_K)}
\end{bmatrix}
$$
$$
(12)
$$

$$
\mathbf{C}_{M \times S} = \begin{bmatrix}
e^{-j\pi \cos(\varphi_1)} & e^{-j\pi \cos(\varphi_2)} & \cdots & e^{-j\pi \cos(\varphi_S)} \\
e^{-j2\pi \cos(\varphi_1)} & e^{-j2\pi \cos(\varphi_2)} & \cdots & e^{-j2\pi \cos(\varphi_S)} \\
\vdots & \vdots & \ddots & \vdots \\
e^{-jM\pi \cos(\varphi_1)} & e^{-jM\pi \cos(\varphi_2)} & \cdots & e^{-jM\pi \cos(\varphi_S)}
\end{bmatrix}
$$
$$
(13)
$$

with $\omega_k = \vartheta_1 + k(\vartheta_2 - \vartheta_1)/K$, $k = 1, 2, \cdots, K$ and

$$
\varphi_s = \begin{cases}
\vartheta_1 s/T_1, & s < \frac{\vartheta_1 K}{\vartheta_2 - \vartheta_1} \\
\vartheta_2 + \frac{(180 - \vartheta_2)(s - \vartheta_1)}{S - T_1}, & \frac{\vartheta_1 K}{\vartheta_2 - \vartheta_1} \leq s < S.
\end{cases} \quad (14)
$$

In this case, our task becomes finding $\mathbf{u}_K$ from $\mathbf{y}_M$.

Denote $\mathbf{b}_M(\omega_k) = [e^{-j\pi \cos(\omega_k)} \quad e^{-j2\pi \cos(\omega_k)} \quad \cdots \quad e^{-jM\pi \cos(\omega_k)}]^T$ as the kth column of $\mathbf{B}_{M \times K}$. Employing the WLS approach, the estimate of u_k, denoted by $\hat{u}_k$, is obtained as

$$
\hat{u}_k = \arg \min_{\tilde{u}_k} (\mathbf{y}_M - \mathbf{b}_M(\omega_k)\tilde{u}_k)^H \mathbf{P}_M^{-1}(\mathbf{y}_M - \mathbf{b}_M(\omega_k)\tilde{u}_k),
$$
$$
(15)
$$

where the weighting matrix $\mathbf{P}_M$ is defined the same as (9). Based on (11), $\mathbf{P}_M$ is now expressed as

$$
\begin{aligned}
\mathbf{P}_M &= E\left\{(\mathbf{B}_{M \times K}\mathbf{u}_K + \mathbf{C}_{M \times S}\mathbf{z}_S)(\mathbf{B}_{M \times K}\mathbf{u}_K + \mathbf{C}_{M \times S}\mathbf{v}_S)^H\right\}, \\
&= \mathbf{B}_{M \times K} E\{\mathbf{u}_K\mathbf{u}_K^H\}\mathbf{B}_{M \times K}^H + \mathbf{C}_{M \times S}E\{\mathbf{v}_K\mathbf{v}_K^H\}\mathbf{C}_{M \times S}^H. \quad (16)
\end{aligned}
$$

From the Appendix, $E\{\mathbf{v}_S\mathbf{v}_S^H\}$ is equal to $\sigma_z^2\mathbf{I}_S$ with σ_z^2 denoting the variance of noise term $\mathbf{v}_K$ and $\mathbf{I}_S$ being the $S \times S$ identity matrix. Therefore, (16) is now

$$
\begin{aligned}
\mathbf{P}_M = \mathbf{B}_{M \times K} \mathrm{diag}\left(E\{|u_1|^2\} \; E\{|u_2|^2\} \; \cdots \; E\{|u_K|^2\}\right) \mathbf{B}_{M \times K}^H \\
+ \sigma_z^2 \mathbf{C}_{M \times S}\mathbf{C}_{M \times S}^H. \quad (17)
\end{aligned}
$$

Here $\mathbf{P}_M$ is still a complicated expression of unknown $\mathbf{u}_K$, therefore, u_k can be estimated iteratively with the $(\ell+1)$th estimate being

$$
\hat{u}_k^{(\ell+1)} = \frac{\mathbf{b}_M^H(\omega_k)\left(\mathbf{P}_M^{(\ell)}\right)^{-1}\mathbf{y}_M}{\mathbf{b}_M^H(\omega_k)\left(\mathbf{P}_M^{(\ell)}\right)^{-1}\mathbf{b}_M(\omega_k)}, \quad k = 1, 2, \cdots, K,
$$
$$
(18)
$$

where

$$
\mathbf{P}_M^{(\ell)} = \mathbf{B}_{M \times K}\mathbf{G}_K^{(\ell)}\mathbf{B}_{M \times K}^H + \left(\hat{\sigma}_z^2\right)^{(\ell)}\mathbf{C}_{M \times S}\mathbf{C}_{M \times S}^H, \quad (19)
$$

with $\mathbf{G}_K^{(\ell)} = \mathrm{diag}\left(|\hat{u}_1^{(\ell)}|^2 \; |\hat{u}_2^{(\ell)}|^2 \; \cdots \; |\hat{u}_K^{(\ell)}|^2\right)$. According to the proof in the Appendix, σ_z^2 and noise variance σ^2 are related by $\sigma_z^2 = \frac{\sigma^2}{L}$, while σ^2 can be computed as [30]:

$$
\left(\hat{\sigma}^2\right)^{(\ell)} = \frac{1}{M}(\mathbf{y}_M - \hat{\mu}^{(\ell)}\mathbf{B}_{M \times K}\hat{\mathbf{u}}_K^{(\ell)})^H(\mathbf{y}_M - \hat{\mu}^{(\ell)}\mathbf{B}_{M \times K}\hat{\mathbf{u}}_K^{(\ell)}),
$$
$$
(20)
$$

where $\hat{\mu}^{(\ell)}$ is the scaling parameter because the value of $\mathbf{u}_K$ may not exactly equal $\{s_p\}_{p=1}^P$. Using the least squares (LS) approach, $\hat{\mu}^{(\ell)}$ is obtained by minimizing

$$
J(\mu) = \left(\mathbf{y}_M - \mu^{(\ell)}\mathbf{B}_{M \times K}\hat{\mathbf{u}}_K^{(\ell)}\right)^H \left(\mathbf{y}_M - \mu^{(\ell)}\mathbf{B}_{M \times K}\hat{\mathbf{u}}_K^{(\ell)}\right).
$$
$$
(21)
$$

Solving (21) yields:

$$\hat{\mu}^{(\ell)} = \frac{\left(\hat{\mathbf{u}}_K^{(\ell)}\right)^H \mathbf{B}_{M \times K}^H \mathbf{y}_M}{\left(\hat{\mathbf{u}}_K^{(\ell)}\right)^H \left(\mathbf{B}_{M \times K}^H \mathbf{B}_{M \times K}\right) \hat{\mathbf{u}}_K^{(\ell)}}. \tag{22}$$

The steps of SIAA I are summarized in Table 1.

TABLE 1. Summary of SIAA I.

(i) Initialize $\{\hat{u}_k^{(0)}\}_{k=1}^K$ as all ones;
(ii) Compute $\mathbf{P}_M^{(\ell)}$, $(\hat{\sigma}_M^2)^{(\ell)}$ using (19)–(22);
(iii) Update $\{\hat{u}_k^{(\ell+1)}\}_{k=1}^K$ using (18);
(v) Repeat Steps (ii)–(iii) until the relative error $\frac{\|\hat{\mathbf{u}}^{(\ell+1)} - \hat{\mathbf{u}}^{(\ell)}\|_2}{\|\hat{\mathbf{u}}^{(\ell+1)}\|_2} < \epsilon$ with ϵ being the tolerance and $\|\ \|_2$ denoting the ℓ_2-norm.

B. SIAA II

Although SIAA I can provide a high-resolution spectrum in a selected frequency range $(\vartheta_1, \vartheta_2]$, the condition that $180/L = (\vartheta_2 - \vartheta_1)/K$ should be satisfied. That is to say, SIAA I is not flexible for arbitrary selective range. In this case, we propose a more general DOA estimator, which is named SIAA II.

Here we still assume that all noise-free signals are located in the interested interval $(\vartheta_1, \vartheta_2]$. According to (2) and with assumption that all signals are in the interested range, the ULA signal model is now expressed as

$$\mathbf{y}_M = \mathbf{B}_{M \times K} \mathbf{w}_K + \mathbf{q}_M, \tag{23}$$

where $\mathbf{B}_{M \times K}$ is defined in (12), $\mathbf{w}_K = [w_1\ w_2\ \cdots\ w_K]^T$ is the spectrum of noise-free signal in $(\vartheta_1, \vartheta_2]$. Here the task of DOA is estimating $\mathbf{w}_K$ from $\mathbf{y}_M$.

The estimate of w_k, referred to as $\hat{w}_k$, can be computed using the WLS approach:

$$\hat{w}_k = \arg \min_{\tilde{w}_k} (\mathbf{y}_M - \mathbf{b}_M(\omega_k) \tilde{w}_k)^H \mathbf{F}_M^{-1} (\mathbf{y}_M - \mathbf{b}_M(\omega_k) \tilde{w}_k), \tag{24}$$

where the weighting matrix $\mathbf{F}_M$ is still the covariance of observed data $\mathbf{y}_M$. According to the definition in (9), we have

$$\begin{aligned}
\mathbf{F}_M &= E\{(\mathbf{B}_{M \times K} \mathbf{s}_K + \mathbf{q}_M)(\mathbf{B}_{M \times K} \mathbf{s}_K + \mathbf{q}_M)^H\}, \\
&= \mathbf{B}_{M \times K} \operatorname{diag}\left(|w_1|^2\ |w_2|^2\ \cdots\ |w_K|^2\right) \mathbf{B}_{M \times K}^H + \sigma^2 \mathbf{I}_M,
\end{aligned} \tag{25}$$

where $\mathbf{I}_M$ is the $M \times M$ identity matrix.

Similarly, (24) is solved in an iterative manner. The $(\ell + 1)$th estimate, namely, $\hat{w}_k^{(\ell+1)}$, is computed as

$$\hat{w}_k^{(\ell+1)} = \frac{\mathbf{b}_M^H(\omega_k)(\mathbf{F}_M^{(\ell)})^{-1} \mathbf{y}_M}{\mathbf{b}_M^H(\omega_k)(\mathbf{F}_M^{(\ell)})^{-1} \mathbf{b}_M(\omega_k)}, \quad k = 1, 2, \cdots, K, \tag{26}$$

where

$$\mathbf{F}_M^{(\ell)} = \mathbf{B}_{M \times K} \mathbf{O}_K^{(\ell)} \mathbf{B}_{M \times K}^H + \left(\hat{\sigma}_M^2\right)^{(\ell)} \mathbf{I}_M, \tag{27}$$

with $\left(\hat{\sigma}_M^2\right)^{(\ell)}$ being

$$(\hat{\sigma}_M^2)^{(\ell)} = \frac{1}{M}(\mathbf{y}_M - \hat{\mu}^{(\ell)} \mathbf{B}_{M \times K} \hat{\mathbf{w}}_K^{(\ell)})^H (\mathbf{y}_M - \hat{\mu}^{(\ell)} \mathbf{B}_{M \times K} \hat{\mathbf{w}}_K^{(\ell)}), \tag{28}$$

$$\mathbf{O}_K^{(\ell)} = \operatorname{diag}\left(|\hat{w}_1^{(\ell)}|^2\ |\hat{w}_2^{(\ell)}|^2\ \cdots\ |\hat{w}_K^{(\ell)}|^2\right), \tag{29}$$

and $\hat{\mu}^{(\ell)}$ is also updated using (22).

Finally, we summarize the steps of SIAA II in Table 2.

TABLE 2. Summary of SIAA II.

(i) Initialize $\{\hat{w}_k^{(0)}\}_{k=1}^K$ as all ones;
(ii) Compute $\mathbf{F}_M^{(\ell)}$, $(\hat{\sigma}_M^2)^{(\ell)}$ using (22)–(29);
(iii) Update $\{\hat{w}_k^{(\ell+1)}\}_{k=1}^K$ using (26);
(v) Repeat Steps (ii)–(iii) until the relative error $\frac{\|\hat{\mathbf{w}}^{(\ell+1)} - \hat{\mathbf{w}}^{(\ell)}\|_2}{\|\hat{\mathbf{w}}^{(\ell+1)}\|_2} < \epsilon$.

C. COMPUTATIONAL COMPLEXITY

The complexity of IAA, SIAA I and SIAA II is investigated in this section. At each iteration, the numbers of multiplications required are $2LM^2 + LM + M^3$, $2KM^2 + 2KM + M^3 + LM$ and $2KM^2 + 3KM + M^3$, respectively. In the proposed schemes, the additional computational cost of $2KM$ is due to the calculation of $\hat{\sigma}^{(\ell)}$ and $\hat{\mu}^{(\ell)}$. That is to say, when the increment of scanning grid is identical among IAA, SIAA I and SIAA II, the proposed ones are more computationally efficient. It is worth pointing that in the case of large number of sensors, fast implementation of SIAA I and SIAA II can be realized according to [24]–[26].

IV. SIMULATION RESULTS

To evaluate the performance of the proposed methods, computer simulations have been conducted. We employ the empirical mean square error (MSE) and absolute bias of $\hat{\varpi}$, defined as $E\{(\varpi - \hat{\varpi})^2\}$ and $|\varpi - E\{\hat{\varpi}\}|$, as the performance metrics. The Cramér-Rao lower bound (CRLB) [31] is included as the benchmark while comparisons with the Capon, APES and MUSIC methods are also provided. The received signal is generated according to (1). For the IAA, Capon, APES and MUSIC estimators, the scanning grid is uniformly with the increment between adjacent points being 1°, while the selective range in the proposed methods is chosen as $\vartheta_1 = 30°$ and $\vartheta_2 = 60°$ with same increment. Therefore, K and L are 30 and 180, respectively. All results are simulated using Matlab running on Intel(R) Core(TM) i7-4790 CPU@3.60GHz and Windows 7 for 1000 Monte Carlo trials with $M = 80$ sensors in ULA.

First, we investigate the estimation performance versus SNR. Here we consider one source located at 41.1° and the three-point parabolic interpolation [32] is utilized to remove the estimation bias. Figures 2 and 3 show the MSE and bias of $\hat{\varpi}$ versus SNR. It is seen that the performance of SIAA I and SIAA II is superior to IAA and Capon estimators, since they can provide reliable performance when SNR < −1 dB. It is noted that the APES fails to estimate $\hat{\varpi}$

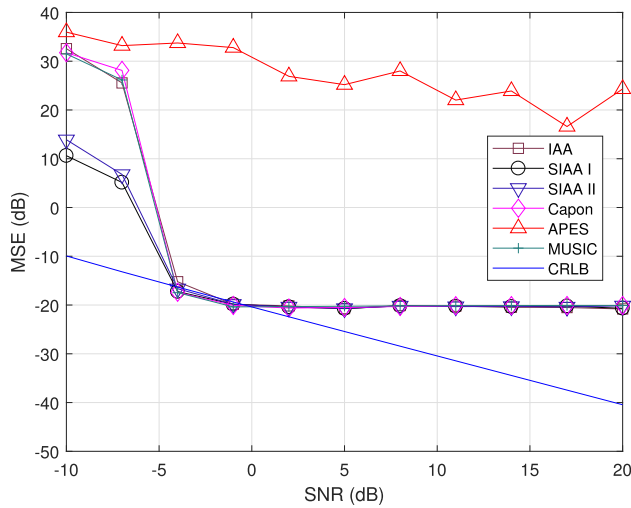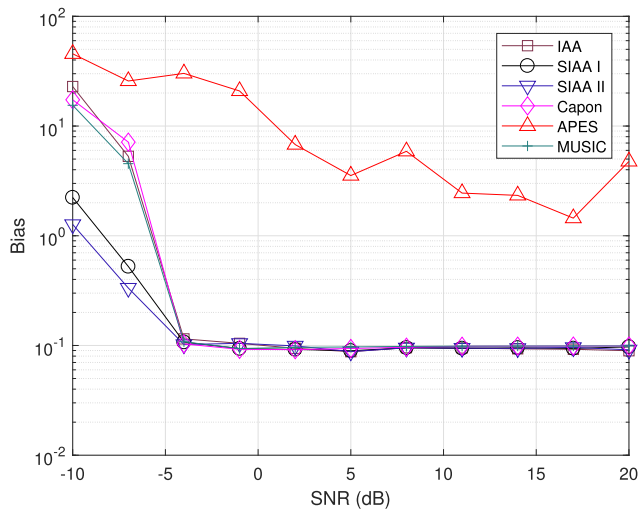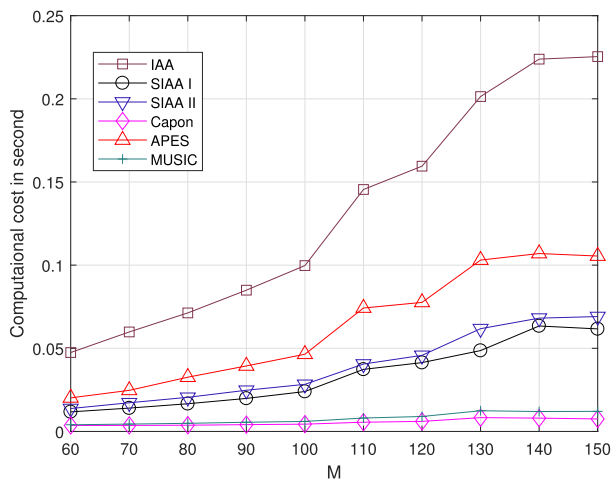**FIGURE 2.** MSE versus SNR.

FIGURE 3. Bias versus SNR.

FIGURE 4. Computational cost versus *M* at SNR = 12 dB.

computational cost. It is indicated that our proposed schemes are significantly faster than IAA and changes slowly as *M* varies.
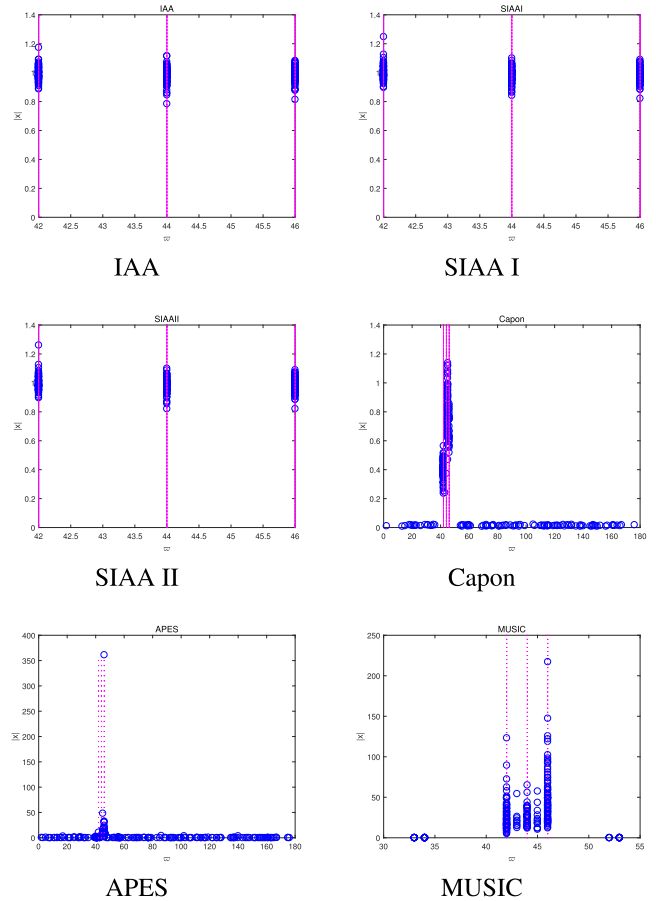

FIGURE 5. Frequency estimates at SNR = 12 dB.

Second, we study the case that all source waveforms are in selective range with SNR = 12 dB and 100 Monte carlo runs are performed. Three closely-spaced uncorrelated sources at 42°, 44° and 46° are considered. It is seen in Figure 5 that all estimates of the IAA and SIAA I and SIAA II locate in (42°, 46°), and they can resolve three clusters around 42°, 44° and 46° clearly. While for the other three conventional estimators, they fail to provide a reliable and high-resolution estimation. This demonstrates that our proposed methods have higher resolvability.

Thirdly, the scenario that not all sources are in the selective range is considered. Here five uncorrelated sources at 16°, 42°, 44°, 68° and 70° are investigated, where only sources at 42° and 44° are our interested signals. The SNR is set to 12 dB and the experiment is based on 1000 independent trials. Figure 6 shows the DOA spectrum of all estimators. It is seen that only IAA can resolve five peaks in the full range while Capon, APES and MUSIC estimators fails to recognize all peaks. Since signals at 42° and 44° are the interested ones, our proposed methods can provide a reliable estimation of them. This result shows that although our
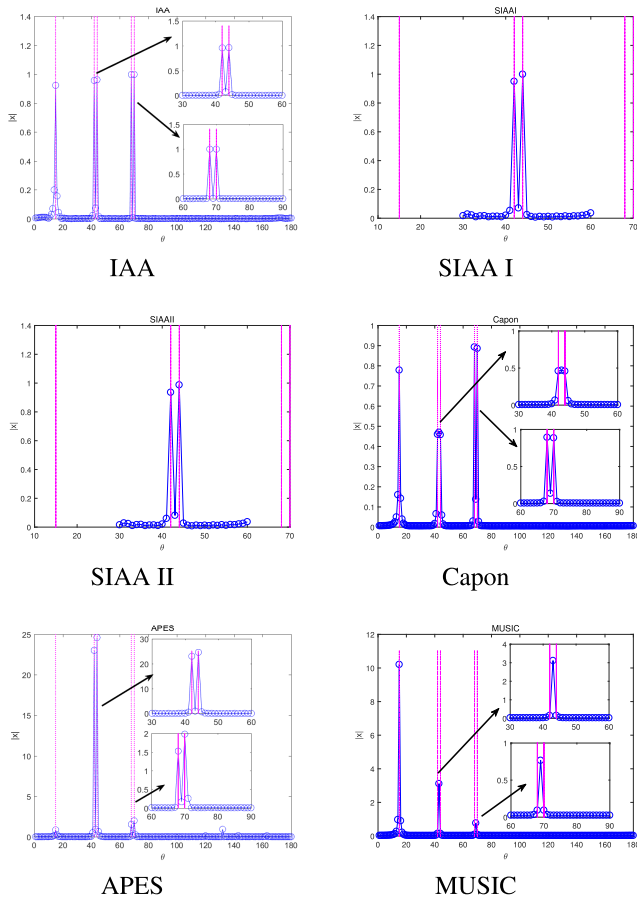
correctly because of the few snapshots. Figure 4 shows the complexity of all estimators versus the number of sensors *M*. The stopwatch timer is employed as the measure of empirical

IAA

SIAA I

SIAA II

Capon

APES

MUSIC

FIGURE 6. DOA spectrum at SNR = 12 dB.

method is developed under the assumption that all sources in the selective range, they can still work on the interested range.

To conclude, the proposed methods, SIAA I and SIAA II, have the same resolution with IAA, while they are more flexible since it can work in any interested azimuth range with one snapshot. On the other hand, they are superior to the APES, Capon and MUSIC, indicating that the SIAA I and SIAA II have higher applicability.

V. CONCLUSION

In this paper, two non-parametric DOA estimators are devised, which have high-resolution with one snapshot observations. With the use of the DOA estimates in any selective azimuth range, two implementation approaches of the covariance matrix are developed, which guarantee the flexibility of the proposed schemes. Simulation results demonstrate the superiority of our estimators over the IAA, APES, Capon and MUSIC methods, in terms of higher resolution and lower computational cost.

APPENDIX
DERIVATION OF $E\{v_S v_S^H\}$

Consider only IID noise term $\mathbf{q} = [q_1 \ q_2 \ \cdots \ q_M]^T$ exist in the observations. According to (2), the noise can be expressed

as

$$\mathbf{q} = \mathbf{A}_{M \times L} \mathbf{z}, \tag{30}$$

where $\mathbf{z} = [z_1 \ z_2 \ \cdots z_L]^T$ can be regarded as the spectrum of the noise and also contains IID random variables following the Gaussian distribution [33]. With the use of definition for variance σ^2 as well as (30), we have

$$\sigma^2 = \frac{1}{M} E\{\mathbf{q}^H \mathbf{q}\}$$
$$= \frac{1}{M} E\{\mathbf{z}^H \left(\mathbf{A}^H \mathbf{A}\right) \mathbf{z}\}. \tag{31}$$

Employing the trace [34] property, (31) can be rewritten as

$$\sigma^2 = \frac{1}{M} \text{trace} \left\{ E\{\mathbf{z}^H \left(\mathbf{A}^H \mathbf{A}\right) \mathbf{z}\} \right\}$$
$$= \frac{1}{M} \text{trace} \left\{ \left(\mathbf{A}^H \mathbf{A}\right) E\{\mathbf{z}^H \mathbf{z}\} \right\}, \tag{32}$$

where trace$\{\mathbf{X}\}$ denotes the trace of $\mathbf{X}$. Since $\mathbf{z}$ are IID Gaussian random variables, according to the definition of trace, (32) is

$$\sigma^2 = \frac{1}{M} \text{trace} \left\{ \left(\mathbf{A}^H \mathbf{A}\right) \sigma_z^2 \right\},$$
$$= \frac{1}{M} ML\sigma_z^2 = L\sigma_z^2, \tag{33}$$

where σ_z^2 is the variance of $\mathbf{z}$.

Similarly, since v_S are also IID random variables outside the interested selective range, we have

$$E\{\mathbf{v}_S \mathbf{v}_S^H\} = \sigma_z^2 \mathbf{I}_S. \tag{34}$$

REFERENCES

[1] X. Wang, M. Huang, C. Shen, and D. Meng, "Robust vehicle localization exploiting two based stations cooperation: A MIMO radar perspective," *IEEE Access*, vol. 6, pp. 48747–48755, 2018.

[2] P. S. Naidu, *Sensor Array Signal Processing*, Boca Raton, FL, USA: CRC Press, 2000.

[3] C. Qian, Y. Shi, L. Huang, and H. C. So, "Robust harmonic retrieval via block successive upper-bound minimization," *IEEE Trans. Signal Process.*, vol. 66, no. 23, pp. 6310–6324, Oct. 2018.

[4] J. Li and P. Stoica, *Robust Adaptive Beamforming*. New York, NY, USA: Wiley, 2005.

[5] Z. Wang, J. Li, and R. Wu, "Time-delay- and time-reversal-based robust capon beamformers for ultrasound imaging," *IEEE Trans. Med. Imag.*, vol. 24, no. 10, pp. 1308–1322, Oct. 2005.

[6] C. Qian, L. Huang, N. D. Sidiropoulos, and H. C. So, "Enhanced PUMA for direction-of-arrival estimation and its performance analysis," *IEEE Trans. Signal Process.*, vol. 64, no. 16, pp. 4127–4137, Aug. 2016.

[7] J. Capon, "High-resolution frequency-wavenumber spectrum analysis," *Proc. IEEE*, vol. 57, no. 8, pp. 1408–1418, Aug. 1969.

[8] P. Handel, P. Stoica, and T. Soderstrom, "Capon method for DOA estimation: Accuracy and robustness aspects," in *Proc. IEEE Winter Workshop Nonlinear Digit. Signal Process.*, Tampere, Finland, Jan. 1993, pp. 1–3.

[9] P. Stoica, P. Händel, and T. Söderström, "Study of Capon method for array signal processing," *Circuits, Syst. Signal Process.*, vol. 14, no. 6, pp. 749–770, Nov. 1995.

[10] X. Wang, L. Wang, X. Li, and G. Bi, "Nuclear norm minimization framework for DOA estimation in MIMO radar," *Signal Process.*, vol. 135, pp. 147–152, Jun. 2017.

[11] D. D. Meng, X. P. Wang, M. X. Huang, and C. Shen, "Reweighted ℓ_1-norm minimization for high resolution DOA estimation under unknown mutual coupling," *Electron. Lett.*, vol. 54, no. 23, pp. 1–2, Sep. 2018.

[12] P. Stoica and A. Nehorai, "MUSIC, maximum likelihood, and Cramér–Rao bound," *IEEE Trans. Acoust., Speech, Signal Process.*, vol. 38, no. 5, pp. 720–741, May 1989.

[13] J. Li and P. Stoica, "An adaptive filtering approach to spectral estimation and SAR imaging," *IEEE Trans. Signal Process.*, vol. 44, no. 6, pp. 1469–1484, Jun. 1996.

[14] D. J. Russell and R. D. Palmer, "Application of APES to adaptive arrays on the CDMA reverse channel," *IEEE Trans. Veh. Technol.*, vol. 53, no. 1, pp. 3–17, Jan. 2004.

[15] P. Stoica, H. Li, and J. Li, "A new derivation of the APES filter," *IEEE Signal Process. Lett.*, vol. 6, no. 8, pp. 205–206, Aug. 1999.

[16] J. G. Proakis, *Digital Communications*. Columbus, OH, USA: McGraw-Hill, 2001.

[17] S. D. Blunt, K. J. Smith, and K. Gerlach, "Doppler-compensated adaptive pulse compression," in *Proc. IEEE Conf. Radar*, Verona, NY, USA, Apr. 2006, pp. 114–119.

[18] J. C. Preisig, "Performance analysis of adaptive equalization for coherent acoustic communications in the time-varying ocean environment," *J. Acoust. Soc. Amer.*, vol. 118, no. 1, pp. 263–278, Jul. 2005.

[19] T. Yardibi, J. Li, P. Stoica, M. Xue, and A. B. Baggeroer, "Source localization and sensing: A nonparametric iterative adaptive approach based on weighted least squares," *IEEE Trans. Aerosp. Electron. Syst.*, vol. 46, no. 1, pp. 425–443, Jan. 2010.

[20] A. Agarwal, A. Kumar, and M. Agrawal, "Iterative adaptive approach to DOA estimation with acoustic vector sensors," in *Proc. OCEANS*, Genoa, Italy, May 2015 pp. 1–8.

[21] E. Gudmundson, A. Jakobsson, J. A. Jensen, and P. Stoica, "Blood velocity estimation using ultrasound and spectral iterative adaptive approaches," *Signal Process.*, vol. 91, no. 5, pp. 1275–1283, 2011.

[22] P. Händel, "Markov-based single-tone frequency estimation," *IEEE Trans. Circuits Syst. II, Analog Digit. Signal Process.*, vol. 45, no. 2, pp. 230–232, Feb. 1998.

[23] T. Soderstrom and P. Stoica, *System Identification*. Englewood Cliffs, NJ, USA: Prentic-Hall, 1989.

[24] M. Xue, L. Xu, and J. Li, "IAA spectral estimation: Fast implementation using the Gohberg–Semencul factorization," *IEEE Trans. Signal Process.*, vol. 59, no. 7, pp. 3251–3261, Jul. 2011.

[25] G.-O. Glentis and A. Jakobsson, "Efficient implementation of iterative adaptive approach spectral estimation techniques," *IEEE Trans. Signal Process.*, vol. 59, no. 9, pp. 4154–4167, Sep. 2011.

[26] G. O. Glentis and A. Jakobsson, "Superfast approximative implementation of the IAA spectral estimate," *IEEE Trans. Signal Process.*, vol. 60, no. 1, pp. 472–478, Jan. 2012.

[27] H. L. Van Trees, *Optimum Array Processing: Part IV of Detection, Estimationand Modulation Theory*. New York, NY, USA: Wiley, 2002.

[28] A. Uncini, *Fundamentals of Adaptive Signal Processing*. New York, NY, USA: Springer, 2015.

[29] Y. Chen, H. C. So, and W. Sun, "ℓ_p-norm based iterative adaptive approach for robust spectral analysis," *Signal Process.*, vol. 94, pp. 144–148, Jan. 2014.

[30] X. Tan, W. Roberts, J. Li, and P. Stoica, "Sparse learning via iterative minimization with application to MIMO radar imaging," *IEEE Trans. Signal Process.*, vol. 59, no. 3, pp. 1088–1101, Mar. 2011.

[31] A. Nehorai and E. Paldi, "Acoustic vector-sensor array processing," *IEEE Trans. Signal Process.*, vol. 42, no. 9, pp. 2481–2491, Sep. 1994.

[32] R. Moddemeijer, "On the determination of the position of extrema of sampled correlators," *IEEE Trans. Signal Process.*, vol. 39, no. 1, pp. 216–219, Jan. 1991.

[33] C. Zhao-Guo and E. J. Hannan, "The distribution of periodogram ordinates," *J. Time Ser. Anal.*, vol. 1, no. 1, pp. 73–82, Jan. 1980.

[34] R. A. Horn, *Matrix Analysis*. Cambridge, U.K.: Cambridge Univ. Press, 2012.

YUAN CHEN was born in Shandong, China. She received the B.Sc. degree from the School of Information Science and Engineering, Shandong University, in 2010, and the Ph.D. degree in electronic engineering from the City University of Hong Kong, in 2015. Since 2015, she has been with the School of Computer and Communication Engineering, University of Science and Technology Beijing, where she is currently an Assistant Professor. Her research interests include statistical signal processing, frequency estimation, machine learning, and their applications.
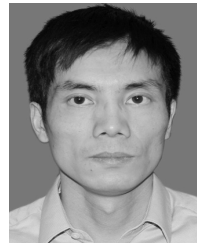
LONG-TING HUANG received the Ph.D. degree from the City University of Hong Kong, in 2016. He is currently a Lecturer with the School of Information Engineering, Wuhan University of Technology. His research interests include multidimensional frequency estimation, array signal processing, and low-rank matrix/tensor completion.
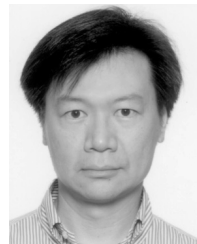
HING CHEUNG SO (S'90–M'95–SM'07–F'15) was born in Hong Kong. He received the B.Eng. degree in electronic engineering from the City University of Hong Kong, in 1990, and the Ph.D. degree in electronic engineering from The Chinese University of Hong Kong, in 1995, where he was a Postdoctoral Fellow, from 1995 to 1996. From 1990 to 1991, he was an Electronic Engineer with the Research and Development Division, Everex Systems Engineering Ltd., Hong Kong. From 1996 to 1999, he was a Research Assistant Professor with the Department of Electronic Engineering, City University of Hong Kong, where he is currently a Professor. His research interests include detection and estimation, fast and adaptive algorithms, multidimensional harmonic retrieval, robust signal processing, source localization, and sparse approximation.

Dr. So was an elected member of the Signal Processing Theory and Methods Technical Committee of the IEEE Signal Processing Society, from 2011 to 2016, where he was the Chair of the Awards Subcommittee, from 2015 to 2016. He was on the Editorial Board of the *IEEE Signal Processing Magazine*, from 2014 to 2017, and the IEEE Transactions on Signal Processing, from 2010 to 2014. He has been on the Editorial Board of *Signal Processing*, since 2010, and *Digital Signal Processing*, since 2011. He was a Lead Guest Editor of the IEEE Journal of Selected Topics in Signal Processing, Special Issue on Advances in Time/Frequency Modulated Array Signal Processing, in 2017.

● ● ●